

This is the Author's Pre-print version of the following article: *Francisco Ignacio Jasso-Robles, María Elisa Gonzalez, Fernando Luis Pieckenstain, José Miguel Ramírez-García, María de la Luz Guerrero-González, Juan Francisco Jiménez-Bremont, Margarita Rodríguez-Kessler, Decrease of Arabidopsis PAO activity entails increased RBOH activity, ROS content and altered responses to Pseudomonas*, *Plant Science*, Volume 292, 2020, 110372, which has been published in final form at: [10.1016/j.plantsci.2019.110372](https://doi.org/10.1016/j.plantsci.2019.110372)

© 2020 This manuscript version is made available under the Creative Commons Attribution-NonCommercial-NoDerivatives 4.0 International (CC BY-NC-ND 4.0) license <http://creativecommons.org/licenses/by-nc-nd/4.0/>

**Title: Decrease of Arabidopsis PAO activity entails increased RBOH activity, ROS content and altered responses to *Pseudomonas***

Francisco Ignacio Jasso-Robles<sup>1</sup> (qfb.ignaciوروبles@gmail.com), María Elisa Gonzalez<sup>2</sup> (mariaelisa@intech.gov.ar), Fernando Luis Pieckenstain<sup>2\*</sup> (pieckenstain@intech.gov.ar), José Miguel Ramírez-García<sup>1</sup> (miguel\_5rmz@hotmail.com), María de la Luz Guerrero-González<sup>3</sup> (luz.guerrero@uaslp.mx), Juan Francisco Jiménez-Bremont<sup>4</sup> (jbremont@ipicyt.edu.mx), Margarita Rodríguez-Kessler<sup>1\*</sup> (mrodriguez@fc.uaslp.mx).

<sup>1</sup>Facultad de Ciencias, Universidad Autónoma de San Luis Potosí (UASLP). Av. Chapultepec 1570, Priv. del Pedregal, 78295, San Luis Potosí, México.

<sup>2</sup>Instituto Tecnológico de Chascomús (INTECH), Universidad Nacional de San Martín (UNSAM), Consejo Nacional de Investigaciones Científicas y Técnicas (CONICET), Avda. Intendente Marino Km 8.2, 7130, Chascomús, Provincia de Buenos Aires, Argentina.

<sup>3</sup>Facultad de Agronomía y Veterinaria, Universidad Autónoma de San Luis Potosí (UASLP). Carretera San Luis-Matehuala Km 14.5, Ejido Palma de la Cruz, 78321, Soledad de Graciano Sánchez, San Luis Potosí, México.

<sup>4</sup>División de Biología Molecular, Instituto Potosino de Investigación Científica y Tecnológica (IPICYT), Camino a la Presa de San José 2055, Lomas 4ª Sección, 78216, San Luis Potosí, México.

\*To whom correspondence should be addressed. E-mail: [mrodriguez@fc.uaslp.mx](mailto:mrodriguez@fc.uaslp.mx) (Telephone number: +52-444-8262300 Ext. 5683); [pieckenstain@intech.gov.ar](mailto:pieckenstain@intech.gov.ar) (Telephone number: +54-2241-430323 Ext. 108).

**Abstract**

Polyamines (PAs) are small aliphatic amines with important regulatory activities in plants. Biotic stress results in changes in PA levels due to *de novo* synthesis and PA oxidation. In *Arabidopsis thaliana* five FAD-dependent polyamine oxidase enzymes (AtPAO1-5) participate in PA back-conversion and degradation. PAO activity generates H<sub>2</sub>O<sub>2</sub>, an important molecule involved in cell signaling, elongation, programmed cell death, and defense responses. In this work we analyzed the role of *AtPAO* genes in the *Arabidopsis thaliana*-*Pseudomonas syringae* pathosystem. *AtPAO1* and *AtPAO2* genes were transcriptionally up-regulated in infected plants. *Atpao1-1* and *Atpao2-1* single mutant lines displayed altered responses to *Pseudomonas*, and an increased susceptibility was found in the double mutant *Atpao1-1 x Atpao2-1*. These polyamine oxidases mutant lines showed disturbed contents of ROS (H<sub>2</sub>O<sub>2</sub> and O<sub>2</sub><sup>•-</sup>) and altered activities of RBOH, CAT and SOD enzymes both in infected and control plants. In addition, changes in the expression levels of *AtRBOHD*, *AtRBOHF*, *AtPRX33*, and *AtPRX34* genes were also noticed. Our data indicate an important role for polyamine oxidases in plant defense and ROS homeostasis.

**Key words:** *Arabidopsis thaliana*-*Pseudomonas syringae* pathosystem; hydrogen peroxide; polyamine oxidases; superoxide anion radical; RBOH enzymes; spermine.

## Abbreviations

Catalase, CAT; Polyamine, PA; Polyamine oxidase, PAO; *Pseudomonas syringae* pv. *tomato*, *Pst*; Putrescine, Put; Respiratory burst oxidase homologue, RBOH; Superoxide dismutase, SOD; Spermidine, Spd; Spermine, Spm.

## 1. Introduction

The *Pseudomonas syringae* pv. *tomato* (*Pst*)-*Arabidopsis* pathosystem has been widely used as a model for studying the interaction of plants with pathogenic bacteria [1]. Disease symptoms caused by *Pst*, appear at final stages of the infection, and are characterized by

regions of localized necrosis surrounded by diffuse chlorosis. After bacterial recognition, complex plant molecular and biochemical responses take place, which involve multiple final immune outputs. Among them, the production of reactive oxygen species (ROS) such as hydrogen peroxide ( $\text{H}_2\text{O}_2$ ) and superoxide anion radical ( $\text{O}_2^{\cdot-}$ ) are critical for plant defense. These ROS are the result of different enzymatic activities, including class III cell wall peroxidases, respiratory burst oxidase homologue (RBOH) proteins, copper-containing amine oxidases (CuAOs), and flavoprotein polyamine oxidases (PAOs), among others [2]. Polyamines (PAs) are low molecular weight aliphatic polycations, with important molecular and physiological functions. In plants, PAs regulate growth, development, and responses to biotic and abiotic stress [3]. The main plant PAs are the diamine putrescine (Put), the triamine spermidine (Spd), and the tetraamines spermine (Spm) and thermospermine (tSpm). Cellular PA levels are tightly regulated through their biosynthesis, catabolism, conjugation, and transport [4]. Members of the CuAO and PAO protein families are responsible of PA catabolism, with different specificities for each polyamine. In *Arabidopsis*, CuAOs are located in the extracellular space and in peroxisomes, and are involved in Put and Spd oxidation, producing aminoaldehydes, ammonia and  $\text{H}_2\text{O}_2$  [5]. PAOs oxidize a variety of higher PAs such as Spd, Spm, tSpm and norspermine by a terminal catabolic pathway, or through PA back-conversion activity. Terminal catabolism of Spd and Spm involves the oxidation of the carbon at the *endo* side of the *N*4-nitrogen, with the concomitant production of aminoaldehydes, 1,3-diaminopropane (1,3-Dap) and  $\text{H}_2\text{O}_2$ . The back-conversion activity oxidizes the carbon at the *exo* side of the *N*4-nitrogen of Spd and Spm producing Put and Spd, respectively, along with 1,3-Dap and  $\text{H}_2\text{O}_2$  [6, 7]. The *Arabidopsis thaliana* genome encodes five PAOs. AtPAO1 and AtPAO5 are localized in the cytosol, while AtPAO2, AtPAO3, and AtPAO4 are peroxisomal enzymes. *AtPAO* gene expression and activity are modulated in a spatio-temporal and tissue specific manner [8, 9], and in response to stress conditions [7, 10, 11, 12]. Accordingly, the levels of PA oxidation products, such as  $\text{H}_2\text{O}_2$ , are also tightly regulated. Hydrogen peroxide is an important signaling molecule that controls several processes in plants, such as cell growth and elongation, stomatal closure, cell-wall stiffening, programmed cell death, as well as biotic and abiotic stress responses [13]. Thus, recent studies have correlated PA catabolism with diverse processes in plant development and stress physiology, and have suggested a

regulatory crosstalk with other enzymes responsible for ROS production, such as RBOH proteins [14].

In *Arabidopsis*, ten genes encoding RBOH proteins have been identified. These transmembrane enzymes are involved in superoxide anion radical ( $O_2^{\bullet-}$ ) production, which can be dismutated into  $H_2O_2$  spontaneously or enzymatically through superoxide dismutase (SOD) activity [15]. The *AtRBOHD* and *AtRBOHF* enzymes are necessary for ROS production in response to pathogen attack and cell death signaling, respectively. In the *Arabidopsis-Pst* interaction, a rapid and transient ROS production in PAMP-triggered immune responses depends on *AtRBOHD* function, and was associated with the regulation of stomatal closure, lignin biosynthesis and callose deposition [15].

In relation to the contribution of  $H_2O_2$  derived from PA oxidation to plant defense, PAO inhibition by 1,19-bis(ethylamino)-5,10,15-triazanonadecane (SL-11061) resulted in increased susceptibility of *Arabidopsis* to *Pseudomonas viridiflava* infection [16]. Therefore, it was suggested that plant protection depends on increased  $H_2O_2$  levels derived from Spm oxidation, implying that PA catabolism is an essential component of the defense response [16]. Nevertheless, the contribution of different *AtPAO* genes in this process has not been estimated so far.

Herein, we analyzed the expression levels and enzymatic activity of *A. thaliana* polyamine oxidases during the interaction with *Pst*. We characterized single and double null mutant lines of cytosolic (*Atpao1-1*) and peroxisomal (*Atpao2-1*) polyamine oxidase genes. These mutants were affected in their response to *Pst*, had altered contents of ROS ( $H_2O_2$  and  $O_2^{\bullet-}$ ) and variations in antioxidant enzyme activities (SOD and Catalase). Accumulation of  $O_2^{\bullet-}$  in *Atpao* mutants can be explained in part by changes in *AtRBOHD* and *AtRBOHF* transcript levels and *AtRBOH* activity. Our data highlight the importance of PAOs in plant defense and their interrelation with other enzymes involved in ROS production and detoxification.

## **2. Materials and methods**

### *2.1. Plant material and growth conditions*

*Arabidopsis thaliana* ecotype Col-0 and T-DNA insertion lines for polyamine oxidase genes, *Atpao1-1* (TAIR: SALK\_013026.56.00.x) and *Atpao2-1* (TAIR: SALK\_049456.42.05.x) (Supplementary Fig. S1A, B) were acquired from the Salk Institute Genomic Analysis Laboratory ([www.signal.salk.edu/cgi-bin/tdnaexpress](http://www.signal.salk.edu/cgi-bin/tdnaexpress)), [17]. The *Atpao1-1*  $\times$  *Atpao2-1* double mutant was obtained by standard genetic crosses. Identification of homozygous lines was performed by PCR (Supplementary Fig. S1A-C), specific primers for *Atpao1-1*, *Atpao2-1* and the T-DNA are depicted on Table S1. Absence of *AtPAO1* and/or *AtPAO2* expression in the *Atpao* T-DNA mutant lines was confirmed by semi-quantitative RT-PCR (Supplementary Fig. S1D; Supplementary Table S1). The *AtEF1 $\alpha$*  (At5g60390) gene was used as reference.

Seeds were surface disinfected for 8 min with 30% sodium hypochlorite (6% free chlorine), and rinsed several times in distilled water. Plants were grown from stratified seeds (2 d at 4°C) on MS 0.5x Petri plates containing 1.5% (w/v) sucrose, 1.2% (w/v) agar, pH 5.7 [18]. All experiments were conducted under controlled conditions in growth chambers under 16/8 h light/dark cycles at 22  $\pm$  2°C.

## 2.2. Bacterial strain, plant inoculation, and estimation of *in planta* bacterial titers

*Pseudomonas syringae* pv. *tomato* strain, DC3000, was cultured at 28°C under constant agitation (150 rpm) in liquid King's B medium. For plant inoculation, bacterial cells were collected by centrifugation, washed three times with 10 mM MgCl<sub>2</sub> pH 7.0, and adjusted to a final concentration of 4x10<sup>8</sup> CFU/mL, as previously described by Gonzalez et al. [16]. Fifteen-day-old seedlings of *A. thaliana* Col-0 and the mutant lines *Atpao1-1*, *Atpao2-1*, and *Atpao1-1*  $\times$  *Atpao2-1* were inoculated with 5  $\mu$ L aliquots of bacterial suspensions on the leaf blade (one per plant) and samples were collected 24, 48 and 72 hpi. Seedlings inoculated with 5  $\mu$ L 10 mM MgCl<sub>2</sub> pH 7.0 were used as controls.

For the estimation of *in planta* bacterial titers, leaves of inoculated plants were surface disinfected with 70% (v/v) ethanol for 2 min and washed three times with 10 mM MgCl<sub>2</sub> pH 7.0. Then, leaves were homogenized in microcentrifuge tubes containing 200  $\mu$ L 10 mM MgCl<sub>2</sub> with a pestle, and 10-fold serial dilutions of the extracts were plated on King's B agar medium. After 24 h of incubation at 28°C, the number of CFU was estimated. For each sample three biological replicates (each consisting of two plants) were analyzed.

Experiments were conducted at least twice with similar results.

### 2.3. RNA isolation and gene expression analysis

Total RNA was isolated using the TRI Reagent® (Sigma-Aldrich). After RNA extraction, DNase I (Thermo Scientific) treatment and first strand cDNA synthesis were performed following previously reported protocols [19]. Gene expression levels were estimated by qRT-PCR using the SsoAdvanced™ Universal SYBR® Green Supermix protocol (BioRad). The oligonucleotides used to amplify each gene are listed in Supplementary Table S1. qPCR thermal cycling conditions consisted of 30 s at 95°C (initial denaturation) and 40 PCR cycles of 10 s at 95°C (denaturation) and 30 s at 60°C (annealing/extension). Melting curves were performed starting at 65°C and gradually increasing the temperature every 0.5°C up to 95°C. The fold change in gene expression relative to control samples was calculated using the  $2^{-\Delta\Delta C_t}$  method [20]. For each sample, three biological replicates were analyzed with their respective technical replicates. Arabidopsis *AtUBQ10* (At4g05320) and *AtEF1 $\alpha$*  were used as reference genes.

### 2.4. Protein extraction

Protein extracts were obtained from 200 mg plant tissues. The extraction buffer used for the determination of AtRBOH and SOD activities contained 200 mM Tris-HCl (pH 8.0; tissue to buffer ratio 1/5, w/v), 1 mM EDTA, 5 mM dithiothreitol (DTT), 1X Halt™ Protease & Phosphatase Inhibitor Cocktail (Thermo Scientific), 10% glycerol and 0.5% Triton X-100 (Sigma-Aldrich). The extraction buffer used for the determination of PAO and catalase (CAT) activities contained 200 mM potassium phosphate buffer (pH 7.0; tissue to buffer ratio 1/5, w/v) and 1 mM phenyl-methyl-sulphonyl-fluoride (PMSF). Protein extracts were centrifuged at 13,000 rpm 20 min at 4°C. Protein concentrations were estimated by the Bradford method using bovine serum albumin as the reference standard [21].

### 2.4. AtRBOH activity

In gel AtRBOH enzymatic assays were performed as described by Carter et al. [22]. Protein extracts (300  $\mu$ g) were resolved electrophoretically in a native 10% polyacrylamide gel at 50 mA. The native gel was washed in 10 mM Tris-HCl (pH 7.4) buffer for 30 min, and then

was incubated in 10 mM Tris-HCl (pH 7.4) buffer supplemented with 0.5 mg/mL nitroblue tetrazolium (NBT, Sigma-Aldrich) and 134  $\mu$ M NADPH (Sigma-Aldrich), until bands were detected. Polyacrylamide gels were scanned using the Molecular Imager PhorosFX System (Bio-Rad). Formazan band intensity was detected with Image J program. RBOH activity was expressed as relative units (RU).

#### *2.6. SOD activity*

Superoxide dismutase activity was determined as described by Azevedo et al. [23]. Protein extracts (300  $\mu$ g) were resolved electrophoretically in a native 8% polyacrylamide gel at 50 mA. Then the gel was rinsed in 50 mM potassium phosphate buffer (pH 7.8) for 30 min. Afterwards, the gel was incubated 30 min in a reaction mixture containing 50 mM potassium phosphate buffer (pH 7.8), 1 mM EDTA, 0.05 mM riboflavine (Sigma-Aldrich), 0.1 mM NBT (Sigma-Aldrich), and 0.3% N,N,N',N'-tetramethylethylenediamine (TEMED). Finally, the gel was washed with distilled water until colorless bands appeared on the purple background. Polyacrylamide gels were scanned using the Molecular Imager PhorosFX System (Bio-Rad). Band intensities were quantified with Image J program. MnSOD, FeSOD and Cu/ZnSOD activities were expressed as relative units (RU).

#### *2.7. Catalase activity*

Catalase activity was determined according to Sahebani and Hadavi [24] with some modifications. The reaction mixture (500  $\mu$ L) contained 10 mM potassium phosphate buffer (pH 7.0), 50  $\mu$ L of protein extract and 3% H<sub>2</sub>O<sub>2</sub> (v/v). Catalase activity was calculated based on the rate of H<sub>2</sub>O<sub>2</sub> decomposition; measured as the decrease in H<sub>2</sub>O<sub>2</sub> absorbance at 240 nm after a one-minute reaction. The molar extinction coefficient ( $\epsilon$ ) of H<sub>2</sub>O<sub>2</sub> at 240 nm (43.6 M<sup>-1</sup>cm<sup>-1</sup>) was used for CAT activity estimation. Enzymatic activity was expressed as U/mg of protein; one CAT unit (U) is defined as the decomposition of 1  $\mu$ mol of H<sub>2</sub>O<sub>2</sub> per minute.

#### *2.8. Determination of polyamine oxidase activity*

PAO activity was determined spectrophotometrically by the formation of a pink adduct

( $\epsilon_{515} = 2.6 \times 10^4 \text{ M}^{-1} \text{ cm}^{-1}$ ) as described by Jasso-Robles et al. [19]. The reaction mixture contained 200 mM potassium phosphate buffer (pH 7.0), 0.06 mg horseradish peroxidase (HRP), 100  $\mu\text{M}$  4-aminoantipyrine (4-AP), 1 mM 3,5-dichloro-2-hydroxybenzenesulphonic acid (DCHBS) in 0.1 mL total volume. The reaction was started by adding 2  $\mu\text{L}$  of 2 mM Spd or Spm as the substrates and incubated for 2 min at 30°C. PAO activity was expressed as nKat/mg protein.

### 2.9. Quantitation of hydrogen peroxide and superoxide anion radical

Hydrogen peroxide ( $\text{H}_2\text{O}_2$ ) and superoxide anion radical ( $\text{O}_2^{\cdot-}$ ) content were determined following the protocols described by Rodríguez and Taleisnik [25]. For  $\text{H}_2\text{O}_2$  estimation, plant material (200 mg) was submerged completely in the reaction mixture (100 mM 4-AP, 1 mM DCHBS and 0.06 mg/mL HRP), vacuum infiltrated for 1 min and incubated for 2 h at 30°C in the dark. The supernatant was collected, clarified by centrifugation at 10,000 rpm for 5 min and measured spectrophotometrically at 515 nm.  $\text{H}_2\text{O}_2$  absorbance was transformed into concentration values using the molar extinction coefficient ( $2.6 \times 10^4 \text{ M}^{-1} \text{ cm}^{-1}$ ).

For  $\text{O}_2^{\cdot-}$  estimation, plant material (200 mg) was submerged in 0.5 mM 3'-[1-[(phenylamino)-carbonyl]-3, 4-tetrazolium](4-methoxy-6-nitro) benzene sulfonic acid hydrate (XTT) solution and vacuum infiltrated for 1 min. Then, plant material was incubated for 5 h at 30°C in the dark. The supernatant was collected, clarified by centrifugation at 10,000 rpm for 5 min and measured spectrophotometrically at 470 nm. Superoxide anion radical absorbance was transformed into concentration values using the molar extinction coefficient ( $2.16 \times 10^4 \text{ M}^{-1} \text{ cm}^{-1}$ ).

### 2.10. Histochemical analysis of ROS

Histochemical detection of  $\text{H}_2\text{O}_2$  and  $\text{O}_2^{\cdot-}$  species was performed in leaf tissues of 15-day-old seedlings. Plant material was vacuum infiltrated for 1 min with 0.1 mg/mL 3,3-diaminobenzidine (DAB) solution for  $\text{H}_2\text{O}_2$  detection as described by Hernandez et al. [26]. After infiltration, plants were incubated 24 h at 25°C in the dark. Then, plant material was boiled at 70°C in 80% ethanol until chlorophyll was no longer visible.

For  $\text{O}_2^{\cdot-}$  detection, plant material was submerged in 122  $\mu\text{M}$  NBT solution and vacuum infiltrated for 1 min as described by Rodríguez and Taleisnik [25]. After infiltration, plants

were incubated 2 h at 30°C in the dark. Finally, chlorophyll was eliminated from plant material as described above. For microscopic observations of H<sub>2</sub>O<sub>2</sub> and O<sub>2</sub><sup>•-</sup> staining, plants were mounted in 1:1:1 (v/v/v) lactic acid:phenol:water solution on a glass slide.

### 2.11. Polyamine quantification

Free PA content was determined in leaf tissues of 15-day-old *Arabidopsis* seedlings at 0, 24, 48 and 72 h after inoculation with *Pst*. PAs were extracted by grinding 50 mg of fresh plant material with 150 µL perchloric acid (5% v/v), kept for 24 h at 4°C in the dark, and then PA extracts were dansylated according to standard protocols [27]. Dansylated PAs were dissolved in 25 µL acetonitrile, and analyzed by reversed-phase HPLC using a Waters 1525 Binary HPLC Pump, and a 2475 Multi λ Fluorescence Detector [27].

### 2.12. Statistical analysis

Experiments consisted of three biological replicates. Results from representative experiments are shown as means ± SE. Statistical differences ( $p \leq 0.05$ ) were determined by Student's T tests or by one-way ANOVA analysis followed by Dunnett's post hoc tests as appropriate using PRISM 5.0b (GraphPad software).

## 3. Results

### 3.1. Polyamine oxidase activity and *AtPAO* gene expression in *Arabidopsis thaliana* seedlings infected with *Pst*

Catabolism of higher PAs, mainly of Spm, by PAO activity has been proposed as an essential component of the plant defense response. In order to determine the contribution of PAO enzymes to the *Arabidopsis-Pst* infection process, Spd and Spm-oxidation activities were evaluated in 15-day-old *A. thaliana* plants (Col-0 ecotype) at different times after inoculation. In control non-inoculated plants, PAO activity gradually diminished from 0 through 72 h for both substrates (Fig. 1A, B). In infected plants, a peak in Spm-oxidation activity was detected 48 hpi (Fig. 1B), while Spd-oxidation activity remained stable throughout the infection process, thus being higher than the activity of non-inoculated controls 48 and 72 hpi (Fig. 1A).

The Arabidopsis *PAO* gene family consists of five members (*AtPAO1-5*), therefore we evaluated the expression profiles of each gene to determine their contribution to the infection process. Among them *AtPAO1*, *AtPAO2* and *AtPAO3* genes were induced 24 hpi (Fig. 1C). This increase in gene expression persisted up to 72 hpi for *AtPAO2*. The *AtPAO3*, *-4* and *-5* genes were down-regulated 48 and 72 hpi (Fig. 1C).

### 3.2. Bacterial titers in polyamine oxidase mutant lines

The increase in *AtPAO1* and *AtPAO2* expression detected in plants inoculated with *Pst* prompted us to investigate the role of these two genes in plant defense. For this purpose, the *Atpao1-1* and *Atpao2-1* mutant lines were acquired from the SALK Institute (see Materials and Methods), and a double mutant line *Atpao1-1 x Atpao2-1* was generated by crossing single mutants (Supplementary Fig. S1). These mutant lines were inoculated with *Pst* and bacterial titers were determined 24, 48 and 72 hpi. Bacterial titers detected in the *Atpao1-1* mutant were lower (4-fold) than those found in the wild-type (WT) *A. thaliana* Col-0 ecotype 72 hpi, suggesting an increased resistance to *Pst* in this mutant line (Fig. 2A). *Atpao2-1* line showed higher bacterial titers than the WT 48 hpi, but a similar behavior to the WT was observed 72 hpi for this mutant line (Fig. 2B). Finally, an increased susceptibility was noticed in the double mutant *Atpao1-1 x Atpao2-1*, as reflected by the higher bacterial titers of this line 72 hpi, as compared to the WT (Fig. 2C).

### 3.3. Polyamine oxidase activity in polyamine oxidase mutant lines infected by *Pst*

The differential responses to *Pst* infection observed for the mutant lines and WT plants could be related to a reduction in PAO activity and the type of PA oxidized by PAOs. In order to test this hypothesis, we analyzed PAO activity in *Atpao1-1*, *Atpao2-1*, and *Atpao1-1 x Atpao2-1* mutant lines, as well as WT Col-0 (Fig. 3). In non-inoculated seedlings, no differences in Spd-oxidation activity were detected between the mutant lines and the WT Col-0 seedlings (Supplementary Fig. S1E). However, when Spm was used as a substrate, non-inoculated seedlings of all the mutants showed a reduction (ca. 50%) of their PAO activity, as compared to WT plants (Supplementary Fig. S1E).

Likewise, PAO activity was also measured in the mutant lines during the infection with *Pst*. An increase in Spd-oxidation activity was observed for all *Atpao* mutant lines 48 hpi, as compared to non-inoculated controls (Fig. 3). In addition, *Atpao1-1* and *Atpao1-1 x*

*Atpao2-1* mutant lines showed augmented Spm-oxidation activity 24 and 48 hpi, as compared to the non-inoculated plants (Fig. 3A, C).

We also compared PAO activity patterns between infected WT and *Atpao* mutant lines (Fig 1A, B and Fig. 3). The most remarkable differences were a reduction in Spd-oxidation activity 72 hpi in the *Atpao1-1* and the *Atpao1-1 x Atpao2-1* mutant lines compared to the WT (Fig. 1A and Fig. 3). Furthermore, Spm-oxidation activity was ca. 2-fold higher in the *Atpao1-1 x Atpao2* mutant line 24 hpi in comparison to the WT; while a reduction in Spm-oxidation activity was noticed in the *Atpao1-1* mutant 48 hpi (Fig. 1B and Fig. 3).

#### 3.4. Free polyamine content in the *Atpao1-1*, *Atpao2-1* and *Atpao1-1 x Atpao2-1* mutant lines in response to *Pst* infection

The alterations in PAO activity detected in the mutant lines could affect the changes in PA levels triggered by bacterial infection. Therefore, PA levels were analyzed in WT Col-0 and *Atpao* mutants infected by *Pst*, and compared to non-inoculated controls (Supplementary Fig. S2). Put content increased in the WT and in the three *Atpao* mutant lines during *Pst* infection (Supplementary Fig. S2A); however, there were no significant differences between them. Spd and Spm levels remained similar to non-inoculated plants; the exception was the *Atpao1-1* mutant in which a reduction in Spm levels was noticed 72 hpi (Supplementary Fig. S2B, C).

#### 3.5. ROS production in *Atpao* mutant lines in response to *Pst* infection

Hydrogen peroxide ( $H_2O_2$ ) is an important molecule involved in signaling and plant defense responses; which is constantly generated from various sources, including PA catabolism [7]. Therefore, we hypothesized single *Atpao1-1* and *Atpao2-1* mutants and the double *Atpao1-1 x Atpao2-1* mutant could have lower  $H_2O_2$  levels than WT plants, and this could in turn have an impact on pathogen resistance. However, contrary to what we expected, significant increases in  $H_2O_2$  levels (ca. 5 and 3-fold, respectively) were observed in *Atpao1-1* and *Atpao2-1* single mutants compared to the WT under control growth conditions (Fig. 4A, 0 hpi).  $H_2O_2$  can be produced through the enzymatic or spontaneous dismutation of the superoxide anion radical ( $O_2^{\bullet-}$ ) [28]. Therefore, in order to evaluate potential sources for the increase in  $H_2O_2$  levels detected in *Atpao1-1* and *Atpao2-1* mutants, we measured the  $O_2^{\bullet-}$  contents under control conditions in the *Atpao* mutant lines.

In this way, *Atpao* mutant lines were found to contain higher  $O_2^{\bullet-}$  levels than WT plants. In particular, *Atpao2-1* showed a 3-fold increment in  $O_2^{\bullet-}$  content (Fig. 5A, 0 hpi).

Furthermore,  $H_2O_2$  and  $O_2^{\bullet-}$  levels were determined at different time-points of infection with *Pst*. In WT plants, a peak in  $H_2O_2$  was detected 24 hpi (Fig. 4A). In the case of  $O_2^{\bullet-}$  content, a gradual increase was noticed during *Pst* infection; the highest level being reached 48 hpi (Fig. 5A). The time course of  $H_2O_2$  and  $O_2^{\bullet-}$  accumulation observed in WT plants was disturbed in the *Atpao* mutant lines infected with *Pst* (Fig. 4A and 5A). Higher  $H_2O_2$  levels were detected 48 and 72 hpi in the *Atpao2-1* mutant line as compared to WT plants (Fig. 4A). Similar  $H_2O_2$  levels were detected 24 hpi in the *Atpao* mutant lines and the WT (Fig. 4A). However, the levels of this metabolite 48 and 72 hpi were significantly lower in the *Atpao1-1* mutant line. The *Atpao1-1 x Atpao2-1* double mutant maintained similar  $H_2O_2$  levels to the WT during *Pst* infection (Fig. 4A).

The three *Atpao* mutant lines and the WT seedlings showed an increase in  $O_2^{\bullet-}$  in response to *Pst* infection (Fig. 5A). Specifically,  $O_2^{\bullet-}$  levels were higher in all the mutant lines than in WT plants 24 hpi (Fig. 5A). The single mutants *Atpao1-1* and *Atpao2-1* still showed higher  $O_2^{\bullet-}$  levels than the WT plants 48 and 72 hpi (Fig. 5A). In particular, a dramatic increase was noticed for *Atpao1-1* mutant 48 hpi, as well as for both the *Atpao1-1* and *Atpao2-1* single mutants 72 hpi, as compared to the WT (Fig. 5A). As opposed to the single *Atpao* mutants, the double *Atpao1-1 x Atpao2-1* mutant showed lower  $O_2^{\bullet-}$  levels than WT plants, both 48 and 72 hpi.

In addition to total  $H_2O_2$  and  $O_2^{\bullet-}$  levels, the spatio-temporal distribution of these ROS in plant tissues was also evaluated, by the histochemical detection using DAB and NBT, respectively. These analyses showed changes in the staining pattern (brown or blue, respectively) during the time-course of infection (Figs. 4B and 5B). At 72 hpi, the WT and the *Atpao1-1* mutant showed a darker  $H_2O_2$  signal through the distal end of the leaf, while the *Atpao2-1* and *Atpao1-1 x Atpao2-1* mutants showed localized spots of  $H_2O_2$  production in the infected leaves (Fig. 4B). The histochemical detection of  $O_2^{\bullet-}$  indicated important changes in the local production of this ROS in infected leaves. At 24 hpi, the three *Atpao* mutant lines analyzed showed that  $O_2^{\bullet-}$  was mainly produced in the borders of leaf blades, in hydathodes; while in WT plants  $O_2^{\bullet-}$  production was observed throughout the whole leaf (Fig. 5B). At 48 and 72 hpi, the  $O_2^{\bullet-}$  signal was still located as spots in the periphery of

infected leaves in the *Atpao* mutant lines, as opposed to the more homogeneous signal detected in the WT (Fig. 5B).

### 3.6. RBOH, SOD and CAT activities in polyamine oxidase mutant lines in response to *Pst* infection

Based on the observation that all *Atpao* mutant lines analyzed showed perturbations in  $\text{H}_2\text{O}_2$  and  $\text{O}_2^{\bullet-}$  levels, we decided to measure the activity of RBOH enzyme responsible for  $\text{O}_2^{\bullet-}$  production, and that of SOD, responsible for  $\text{O}_2^{\bullet-}$  dismutation into  $\text{H}_2\text{O}_2$  [28]. As observed in figure 6A, under control conditions RBOH activity was higher in the *Atpao2-1* and *Atpao1-1 x Atpao2-1* mutant lines than in the WT. Thus, the expression of the *AtRBOHD* and *AtRBOHF* genes was measured in non-inoculated plants (0 hpi). Both *AtRBOHD* and *AtRBOHF* genes were up-regulated in the *Atpao2-1* mutant line, while down-regulation was noticed in the *Atpao1-1 x Atpao2-1* mutant (Supplementary Fig. S3A, B). In addition, the expression levels of *AtPRX33* and *AtPRX34*, which encode extracellular peroxidases that also contribute to  $\text{H}_2\text{O}_2$  generation, were measured in control non-inoculated plants. Both genes were up-regulated in the *Atpao2-1* mutant (Supplementary Fig. S3C, D), while only the expression of *AtPRX34* showed an increase in the double mutant line *Atpao1-1 x Atpao2-1* (Supplementary Fig. S3D). The expression of *AtPRX34*, on its part, was decreased in the *Atpao1-1* mutant (Supplementary Fig. S3D).

We also measured in-gel RBOH activity in infected plants. At 24 and 48 hpi, the three *Atpao* mutant lines had higher RBOH activity than the WT (Fig. 6B and C, respectively), while all the lines showed similar activity to the WT 72 hpi (Fig. 6D). The *AtRBOHD* and *AtRBOHF* expression levels were induced in the *Atpao2-1* and *Atpao1-1 x Atpao2-1* mutant lines 72 hpi (Supplementary Fig. S3A, B). In addition, the expression of *AtPRX33* and *AtPRX34* genes were augmented in the *Atpao1-1* mutant 72 hpi; while down-regulation of *AtPRX34* was observed in the double mutant line *Atpao1-1 x Atpao2-1* (Supplementary Fig. S3C, D).

Furthermore, we measured the activity of antioxidant enzymes such as catalase (CAT) and superoxide dismutase (SOD) in WT and *Atpao* mutant lines. Non-inoculated *Atpao2-1* and *Atpao1-1 x Atpao2-1* mutant lines showed higher CAT activity than the WT (Fig. 7A). During the interaction with *Pst*, CAT activity of the *Atpao1-1* and *Atpao2-1* mutant lines

was similar to that of WT seedlings when analyzed 24 hpi; nonetheless a reduction was observed in the double mutant line (Fig. 7A). Furthermore, an increment in CAT activity was noticed 48 hpi in the *Atpao1-1* and the *Atpao1-1 x Atpao2-1* mutant lines. This increment persisted in the *Atpao1-1* mutant 72 hpi (Fig. 7A). In the case of SOD, it was found that Mn-SOD activity was reduced in non-inoculated seedlings of the *Atpao2-1* and the *Atpao1-1 x Atpao2-1* mutant lines, as compared to WT Col-0 (Fig. 7B). The activity of the other SOD isoforms (Fe-SOD and Zn/Cu-SOD) was similar between non-inoculated seedlings of the *Atpao* mutant lines and the WT (Fig. 7B). When plants were inoculated with *Pst*, the *Atpao1-1* and the *Atpao1-1 x Atpao2-1* mutant lines showed an increase in the activity of the Mn-SOD and Fe-SOD isoforms, while the *Atpao2-1* mutant line responded in a similar way as the WT (Fig. 7C).

#### 4. Discussion

The study of plant PA catabolism mediated by PAO enzymes has increased in the last few years, indicating an important contribution of PAO function in plant development and in biotic and abiotic stress responses [11, 12, 16, 29, 30, 31]. It has been suggested that H<sub>2</sub>O<sub>2</sub> formed due to higher PA oxidation by PAO enzymes acts as a central signaling molecule that mediates PA function and modulates the interrelation of PAs with other signaling pathways. Hydrogen peroxide is an important second messenger that regulates gene expression and participates in diverse processes such as cell wall stiffening, lignification, programmed cell death, and defense. Several lines of evidence point that Spm oxidation and H<sub>2</sub>O<sub>2</sub> production through PAO activity play an important role in the onset of host and non-host hypersensitive responses involved in plant defense [32, 33].

Herein we evaluated the contribution of Arabidopsis PA catabolism in the interaction with the hemibiotrophic bacterium *Pst*. As a first approach, we determined the expression levels of the *AtPAO* genes at different time-points of infection with *Pst* and found that *AtPAO1* and *AtPAO2* genes were induced in 15-day-old Arabidopsis seedlings. These genes encode intracellular enzymes located in the cytosol (*AtPAO1*) and peroxisome (*AtPAO2*). The above-mentioned results are in line with previous observations by Lou et al. [34], who found *AtPAO1* and *AtPAO2* transcripts to be accumulated in leaves of 3-week-old Arabidopsis plants 24 hpi with *Pst*. Transcriptional regulation of *PAO* genes has been

observed in different plant-pathogen interactions. For example, the *ZmPAO1* gene, which encodes an extracellular enzyme, was highly induced in maize tumors induced by *Ustilago maydis* [19]. In cotton cultivars resistant to *Verticillium dahliae*, the expression of the *GhPAO* gene was strongly induced 12 hpi [35]. These studies, as well as the data hereby presented, highlight the importance of *PAO* gene expression in response to pathogens that deploy different pathogenesis strategies (biotrophic, hemibiotrophic and necrotrophic); in particular *AtPAO1* and *AtPAO2* genes in the Arabidopsis-*Pseudomonas* pathosystem.

In addition to changes in gene expression, we also observed changes in PAO activity in *A. thaliana* Col-0 seedlings infected with *Pst*. At early time points of infection (24 hpi), a drop in Spm-oxidation activity was detected and afterwards, an increment was noticed 48 hpi. A similar same behavior was reported for the cotton-*V. dahliae* interaction [35]. It is well known that PAO activity contributes to fine-tuning PA levels through the back-conversion pathway in Arabidopsis [36, 37], a process that could favor Put buildup. We observed an important accumulation of Put in *A. thaliana* leaves during *Pst* infection, while no significant changes in higher PAs (Spd and Spm) content were evident. Thus, we hypothesize that the rise in PAO activity noticed in Arabidopsis seedlings 48 hpi with *Pst* might also be responsible for Put increments in infected tissues through full back-conversion activity. On the other hand, it is well known that increases in ADC activity lead to Put biosynthesis at early time-points of the Arabidopsis-*P. viridiflava* interaction [38]. An increase in Put content was detected in tomato plants infected by *Pst*; this increment was associated with bacterial Put excretion during plant colonization [39]. Therefore, increments in Put levels in infected plants could be derived from different sources, such as *de-novo* biosynthesis, PA back-conversion activity and the contribution of Put from bacterial origin. The role of Put in plant defense was recently discussed, and this diamine was proposed as an important inducer of pathogen associated molecular pattern (PAMP)-triggered immunity (PTI) in the Arabidopsis-*Pst* interaction, playing important roles in callose deposition and transcriptional regulation of PTI marker genes [40].

The role of *AtPAO1* and *AtPAO2* genes in the Arabidopsis-*Pseudomonas* interaction was assessed using single and double mutants of these genes. The *Atpao1-1*, *Atpao2-1* and *Atpao1 x Atpao2-1* mutant lines were affected in their response to *Pst* (Fig. 2), and were characterized by reduced Spm-oxidation activity (Supplementary Fig. S1E). In accordance,

previous *in vitro* studies indicated that Spm is preferred to Spd as a substrate for AtPAO1 and AtPAO2 [36, 37]. In a previous work, Gonzalez et al. [16] demonstrated that elevated Spm levels and its degradation through PAO enzymes is important for the defense against *Pseudomonas*. Therefore our data reinforce the importance of specific PA degradation (mainly Spm) in plant defense.

Furthermore, we determined H<sub>2</sub>O<sub>2</sub> content in the *Atpao* mutant lines, an important product of PA catabolism that participates in cell signaling and defense. *Atpao* mutants could be expected to have lower H<sub>2</sub>O<sub>2</sub> than WT plants, as a consequence of reduced PA oxidation. However the *Atpao* mutants analyzed had higher H<sub>2</sub>O<sub>2</sub> and O<sub>2</sub><sup>•-</sup> levels than WT plants. Increments in O<sub>2</sub><sup>•-</sup> concentration were already reported in the Arabidopsis *Atpao3* mutant line [14]. On its part, other previous works detected no significant differences in H<sub>2</sub>O<sub>2</sub> content between the *Atpao5-3* mutant and WT plants [41, 42]. Besides, inhibition of PAO activity in wheat root segments with 1,8-diaminooctane resulted in O<sub>2</sub><sup>•-</sup> accumulation [43]. In our study, H<sub>2</sub>O<sub>2</sub> and O<sub>2</sub><sup>•-</sup> contents of the *Atpao1-1 x Atpao2-1* double mutant line were similar to those of WT seedlings. Conversely, a reduction in H<sub>2</sub>O<sub>2</sub> levels was reported for the *Atpao1 x Atpao5* double mutant, which lacks cytosolic PAOs [41]. Differences in ROS contents exhibited by these *Atpao* double mutant lines can probably be attributed to the different subcellular localization of the PAO enzymes. Our present data and those works by other authors cited above indicate that loss of function of *PAO* genes as well as PAO inhibition with specific inhibitors cause modifications of ROS contents; thus, demonstrating that PAOs are important for ROS homeostasis.

Hydrogen peroxide generation by PA catabolism is considered as part of the mechanisms by which plants defend themselves against pathogens [44]. In the case of the *Atpao1-1* mutant, the higher basal contents of H<sub>2</sub>O<sub>2</sub> and O<sub>2</sub><sup>•-</sup> could be one of the features related with the resistant phenotype exhibited by this line, as well as the reduction of H<sub>2</sub>O<sub>2</sub> contents 48 and 72 hpi. However, the *Atpao2-1* that also had higher basal ROS contents, behaved as the WT. As previously mentioned, the *Atpao* mutant lines analyzed in this study were affected in the function of cytosolic and/or peroxisomal PAOs. Thus, the differential responses of each mutant line to *Pst* infection suggest that the subcellular site at which PA oxidation occurs could affect plant defense. Then, we hypothesize that not only the increase of ROS levels derived from PAO activity, but also the specific sites of ROS production by different

PAO isoforms are key aspects for the plant defense response. For instance, it has been documented that the threshold of apoplastic PA oxidation can trigger signaling events or the execution of programmed cell death in response to diverse stress conditions [12]. Besides, it has been proposed that PA back-conversion in peroxisomes and the concomitant generation of H<sub>2</sub>O<sub>2</sub> has mainly a role in signaling, perhaps by modulating the activity of Ca<sup>2+</sup> channels. In accordance, Sewelam et al. [45] demonstrated that the site-specific generation of H<sub>2</sub>O<sub>2</sub> in organelles (chloroplast, peroxisome, or both of them) was responsible for differential gene expression profiles and cellular responses. In our study, we observed differential patterns of ROS localization in infected leaves of *Atpao* mutant lines as compared to WT leaves. Perhaps the spatial changes in ROS could differentially affect signaling and defense responses in the *Atpao* mutant lines.

The increase in O<sub>2</sub><sup>•-</sup> levels detected in the *Atpao* mutant lines could be responsible for H<sub>2</sub>O<sub>2</sub> accumulation. It is well known that, O<sub>2</sub><sup>•-</sup> can be produced from molecular oxygen by the action of RBOH enzymes. Interestingly, the *Atpao1-1*, *Atpao2-1* and the *Atpao1-1 x Atpao2-1* lines showed increased RBOH activity that could explain in part the increments in O<sub>2</sub><sup>•-</sup> content. In a similar way, the loss-of-function of *AtPAO3* resulted in increased O<sub>2</sub><sup>•-</sup> production by the NADPH-oxidase, although not of H<sub>2</sub>O<sub>2</sub> [14]. In the *Atpao2-1* mutant, the increment in *AtRBOHD* and *AtRBOHF* expression might be responsible of the augmented RBOH activity detected in this line. On its part, the increments in RBOH activity detected in the *Atpao1-1* and the *Atpao1-1 x Atpao2-1* mutant lines could be related to the expression of other members of the *AtRBOH* family, which were not measured in the present work. We focused on the well-studied *AtRBOHD* and *AtRBOHF* genes, which encode RBOH isoforms well known to participate in defense against pathogens [28, 46]. In infected seedlings of the *Atpao2-1* and the *Atpao1-1 x Atpao2-1* mutant lines, the *AtRBOHD* and *AtRBOHF* genes were induced in response to *Pseudomonas* 72 hpi. However, the double mutant line was more susceptible to *Pst* infection than the WT; this observation suggests that PAO and RBOH enzymatic activities are required for the defense response. The extracellular class III peroxidases PRX33 and PRX34 have also been linked to ROS production and defense responses against pathogen infection [47]. In the case of the *Atpao1-1* mutant, the increased *AtPRX33* and *AtPRX34* expression levels detected in infected seedlings could also be associated with enhanced disease resistance.

SOD and CAT are important members of the enzymatic antioxidant system and are required for the maintenance of ROS homeostasis in the cell [48]. Superoxide dismutase enzymes convert the anion radical  $O_2^{\bullet-}$  into  $H_2O_2$ , which can be further detoxified by CAT in the peroxisome [48]. As already mentioned above, the  $O_2^{\bullet-}$  content increased mainly in the *Atpao2-1* single mutant line, in which the Mn-SOD activity was diminished. Therefore we hypothesize that the increments in  $O_2^{\bullet-}$  in the *Atpao2-1* mutant could be a result of reduced detoxification by Mn-SOD in organelles (peroxisomes or mitochondria), yet, further work is needed to address this issue.

CAT enzymatic activity was higher in the *Atpao2-1* and *Atpao1-1 x Atpao2-1* mutant lines. Likewise, in the *Atpao1 x Atpao5* double mutant line a higher CAT activity was reported [41]. Recently, we found that down-regulation of ADC activity in Arabidopsis leads to increments in ROS, diminution in *AtCat2* gene expression and diminution in CAT activity [49]. On its part, the exogenous application of  $H_2O_2$  to Arabidopsis leaves was shown to increase CAT activity [50]. Thus, the increase in CAT activity exhibited by *Atpao* mutants could be the result of the enhanced  $H_2O_2$  levels exhibited by these lines.

It is well known that changes in salicylic acid (SA) concentrations occur during the Arabidopsis-*Pst* interaction [51]; and that SA signaling conduces to CAT activity inhibition, thus favoring  $H_2O_2$  accumulation [52]. During *Pst* infection, CAT activity gradually diminished with disease progression in both the WT and the *Atpao* mutant lines, nevertheless a slightly higher CAT activity was detected 48 and 72 hpi in the *Atpao1-1* mutant. Moreover, higher Mn-SOD and Fe-SOD activities were found in the *Atpao1-1* mutant line. Perhaps the increments in ROS and antioxidant activities of CAT and SOD enzymes confer *Atpao1-1* an advantage in the defense response, taking into account the enhanced resistance of this line to *Pst* infection. In summary, alterations in the activity of antioxidant enzymes (CAT and SOD) in *Atpao* mutants could be partly due to ROS increments, although other regulatory mechanisms mediated by perturbations in hormonal contents (i.e. SA) and other signaling pathways might also be involved.

## **Conclusion**

Alterations in PA catabolism affect the levels of ROS and the activities of the RBOH and CAT enzymes that compromise the defense of the plant, suggesting a link between PA catabolism (mainly of Spm) and other enzymes involved in ROS homeostasis in plants. In

figure 8, we propose a model for the participation of PA catabolism in the Arabidopsis-*Pst* interaction. First, *Pseudomonas* perception by plant receptors conduces to the activation of enzymes (RBOH) and MAPK-mediated signaling pathways that influence ROS production, gene expression and the synthesis of defense response molecules (i.e. PAs) [11, 53, 54, 55]. Among them, *AtPAO1* and *AtPAO2* genes are up-regulated, and the encoded enzymes contribute to higher PA oxidation in the cytosol (*AtPAO1*) and the peroxisome (*AtPAO2*) by terminal catabolism or full back-conversion activity, respectively. Both PA catabolic pathways conduce to H<sub>2</sub>O<sub>2</sub> production; therefore, PAO activity could impact differentially on gene expression and defense responses depending on the intracellular site of H<sub>2</sub>O<sub>2</sub> generation. On the other hand, we hypothesize that PAO enzymes might contribute to increase Put levels through Spm full back-conversion activity. Put accumulation is a well-reported feature of Arabidopsis-*Pseudomonas* interaction, and can also be achieved by *de-novo* biosynthesis [38] as well as by bacterial Put excretion during plant colonization [39]. In the case of the *Atpao* mutants, the levels of Put still increase. However, diminution of cytosolic and peroxisomal Spm oxidation in the *Atpao1-1* and *Atpao2-1* single and double mutants, affect ROS content and homeostasis. In particular, the production of O<sub>2</sub><sup>•-</sup> derived from RBOH activity, and the consequent accumulation of H<sub>2</sub>O<sub>2</sub> become evident. Therefore, we propose that intracellular Spm oxidation by PAOs can negatively regulate RBOH activity in WT seedlings, by an unknown mechanism that could involve H<sub>2</sub>O<sub>2</sub> signaling.

### **Conflict of interest.**

The authors declare there is no conflict of interest.

### **Author contributions**

FIJR, JMRG, MEG and MLGG performed the experimental work and analyzed the data; MEG, FLP, JFJB, and MRK conceived and designed the research programme; FLP and MRK obtained funding; and all authors commented on the results, contributed and approved to the manuscript.

### **Acknowledgements**

This work was financially supported by CONACYT (Investigación Ciencia Básica 2011-169509), Fondo de Cooperación Bilateral México-Argentina (2012-190390), Agencia Nacional de Promoción Científica y Tecnológica (PICT2014-3286) and CONICET (PIP 11220150100903).

## References

- [1] X.F. Xin, S.Y. He, *Pseudomonas syringae* pv. *tomato* DC3000: A model pathogen for probing disease susceptibility and hormone signaling in plants, *Annu. Rev. Phytopathol.* 51 (2013) 473–498.
- [2] C. Waszczak, M. Carmody, J. Kangasjärvi, Reactive oxygen species in plant signaling, *Annu. Rev. Plant Biol.* 69 (2018) 1–28.
- [3] A.F. Tiburcio, T. Altabella, M. Bitrián, R. Alcázar, The roles of polyamines during the lifespan of plants: from development to stress, *Planta* 240 (2014) 1–18.
- [4] K. Baron, C. Stasolla, The role of polyamines during *in vivo* and *in vitro* development, *Vitr. Cell. Dev. Biol. Plant* 44 (2008) 384–395.
- [5] J. Planas-Portell, M. Gallart, A.F. Tiburcio, T. Altabella, Copper-containing amine oxidases contribute to terminal polyamine oxidation in peroxisomes and apoplast of *Arabidopsis thaliana*, *BMC Plant Biol.* 13 (2013) 109.
- [6] P.N. Moschou, M. Sanmartin, A.H. Andriopoulou, E. Rojo, J.J. Sanchez-Serrano, K.A. Roubelakis-Angelakis, Bridging the gap between plant and mammalian polyamine catabolism: a novel peroxisomal polyamine oxidase responsible for a full back-conversion pathway in *Arabidopsis*, *Plant Physiol.* 147 (2008) 1845–1857.
- [7] P.N. Moschou, J. Wu, A. Cona, P. Tavladoraki, R. Angelini, K.A. Roubelakis-Angelakis, The polyamines and their catabolic products are significant players in the turnover of nitrogenous molecules in plants, *J. Exp. Bot.* 63 (2012) 5003–5015.
- [8] Y. Takahashi, R. Cong, G.H.M. Sagor, M. Niitsu, T. Berberich, T. Kusano, Characterization of five polyamine oxidase isoforms in *Arabidopsis thaliana*, *Plant Cell Rep.* 29 (2010) 965–995.
- [9] P. Fincato, P.N. Moschou, A. Ahou, R. Angelini, K.A. Roubelakis-Angelakis, R. Federico, P. Tavladoraki, The members of *Arabidopsis thaliana* PAO gene family exhibit distinct tissue- and organ-specific expression pattern during seedling growth and flower development, *Amino Acids* 42 (2012) 831–841.
- [10] R. Angelini, A. Tisi, G. Rea, M.M. Chen, M. Botta, R. Federico, A. Cona, Involvement of polyamine oxidase in wound healing, *Plant Physiol.* 146 (2008) 162–177.

- [11] J.F. Jimenez-Bremont, M. Marina, M.L. Guerrero-González, F.R. Rossi, D. Sánchez-Rangel, M. Rodríguez-Kessler, O.A. Ruíz, A. Gárriz, Physiological and molecular implications of plant polyamine metabolism during biotic interactions, *Front. Plant Sci.* 5 (2014) 1–14.
- [12] W. Wang, K. Paschalidis, J. C. Feng, J. Song, J. H. Liu, Polyamine catabolism in plants: a universal process with diverse functions, *Front. Plant Sci.* 10 (2019) 561.
- [13] I. Ślesak, M. Libik, B. Karpinska, S. Karpinski, Z. Miszalski, The role of hydrogen peroxide in regulation of plant metabolism and cellular signalling in response to environmental stresses, *ACTA Biochim. Pol. Ed.* 54 (2007) 39–50.
- [14] E.A. Andronis, P.N. Moschou, I. Toumi, K.A. Roubelakis-Angelakisis, Peroxisomal polyamine oxidase and NADPH-oxidase cross-talk for ROS homeostasis which affects respiration rate in *Arabidopsis thaliana*, *Front. Plant Sci.* 5 (2014) 132.
- [15] Y. Liu, C. He, Regulation of plant reactive oxygen species (ROS) in stress responses: learning from AtRBOHD, *Plant Cell Rep.* 35 (2016) 995–1007.
- [16] M.E. Gonzalez, F. Marco, E.G. Minguet, P. Carrasco-Sorli, M.A. Blázquez, J. Carbonell, O.A. Ruiz, F.L. Pieckenstain, Perturbation of *spermine synthase 1* gene expression and transcript profiling provide new insights on the role of the tetraamine spermine in *Arabidopsis thaliana* defense against *Pseudomonas viridiflava*, *Plant Physiol.* 156 (2011) 2266–2277.
- [17] J.M. Alonso, A.N. Stepanova, T.J. Lisse, C.J. Kim, H. Chen, P. Shinn, others, Genome-wide insertional mutagenesis of *Arabidopsis thaliana*, *Science* 301 (2003) 653–657.
- [18] T. Murashigue, F. Skoog, A revised medium for rapid growth and bio assays with tobacco tissue cultures, *Physiol. Plant.* 15 (1962) 473–497.
- [19] F.I. Jasso-Robles, J.F. Jiménez-Bremont, A. Becerra-Flora, M. Juárez-Montiel, M. E González, F.L. Pieckenstain, R.F. García de la Cruz, M. Rodríguez-Kessler, Inhibition of polyamine oxidase activity affects tumor development during the maize-*Ustilago maydis* interaction, *Plant Physiol. Biochem.* 102 (2016) 115–124.
- [20] K.J. Livak, T.D. Schmittgen, Analysis of relative gene expression data using real-time quantitative PCR and the 2<sup>-</sup>[-Delta Delta C(T)] method, *Methods* 25 (2001) 402–408.

- [21] M.M. Bradford, A rapid and sensitive method for the quantitation of microgram quantities of protein utilizing the principle of protein-dye binding, *Anal. Biochem.* 72 (1976) 248–254.
- [22] C. Carter, R. Healy, N.M. O'Tool, S.M.S. Naqvi, G. Ren, S. Park, G.A. Beattie, H.T. Horner, R.W. Thornburg, Tobacco nectaries express a novel NADPH oxidase implicated in the defense of floral reproductive tissues against microorganisms, *Plant Physiol.* 143 (2007) 389–399.
- [23] R.A. Azevedo, R.M. Alas, R.J. Smith, P.J. Lea, Response of antioxidant enzymes to transfer from elevated carbon dioxide to air and ozone fumigation, in the leaves and roots of wild-type and a catalase-deficient mutant of barley, *Physiol. Plant.* 104 (1998) 280–292.
- [24] N. Sahebani, N. Hadavi, Induction of H<sub>2</sub>O<sub>2</sub> and related enzymes in tomato roots infected with root knot nematode (*M. javanica*) by several chemical and microbial elicitors, *Biocontrol Sci. Technol.* 19 (2009) 301–313.
- [25] A.A. Rodríguez, E.L. Taleisnik, Determination of reactive oxygen species in salt-stressed plant tissues, in: *Plant Salt Toler.*, Springer, 2012: p.p. 225–236.
- [26] J.A. Hernández, M.A. Ferrer, A. Jiménez, A.R. Barceló, F. Sevilla, Antioxidant systems and O<sub>2</sub><sup>-</sup>/H<sub>2</sub>O<sub>2</sub> production in the apoplast of pea leaves. Its relation with salt-induced necrotic lesions in minor veins, *Plant Physiol.* 127 (2001) 817–831.
- [27] M. Marcé, D. Brown, T. Capell, X. Figueras, A. Tiburcio, Rapid high-performance liquid chromatographic method for the quantitation of polyamines as their dansyl derivatives: application to plant and animal tissues, *J. Chromatogr. B. Biomed. Sci. Appl.* 666 (1995) 329–335.
- [28] M.A. Torres, J.L. Dangel, J.D.G. Jones, Arabidopsis gp91<sup>phox</sup> homologues AtrbohD and AtrbohF are required for accumulation of reactive oxygen species intermediates in the plant defense response, *Proc. Natl. Acad. Sci.* 99 (2002) 517–522.
- [29] A.A. Rodríguez, S.J. Maiale, A.B. Mendez, O.A. Ruiz, Polyamine oxidase activity contributes to sustain maize leaf elongation under saline stress, *J. Exp. Bot.* 60 (2009) 4249–4262.
- [30] J. Wu, Z. Shang, J. Wu, X. Jiang, P.N. Moschou, W. Sun, K.A. Roubelakis-Angelakis, S. Zhang, Spermidine oxidase-derived H<sub>2</sub>O<sub>2</sub> regulates pollen plasma membrane

hyperpolarization-activated  $\text{Ca}^{2+}$  permeable channels and pollen tube growth, *Plant J.* 63 (2010) 1042–1053.

[31] T. Kusano, D.W. Kim, T. Liu, T. Berberich, Polyamine catabolism in plants, in: *Polyamines*, Springer, 2015: pp. 77–80.

[32] Y. Takahashi, T. Berberich, A. Miyazaki, S. Seo, Y. Ohashi, T. Kusano, Spermine signalling in tobacco: activation of mitogen-activated protein kinases by spermine is mediated through mitochondrial dysfunction, *Plant J.* 36 (2003) 820–829.

[33] P.N. Moschou, P.F. Sarris, N. Skandalis, A.H. Andriopoulou, K.A. Paschalidis, N.J. Panopoulos, K.A. Roubelakis-Angelakis, Engineered polyamine catabolism preinduces tolerance of tobacco to bacteria and oomycetes, *Plant Physiol.* 149 (2009) 1970–1981.

[34] Y.-R. Lou, M. Bor, J. Yan, A.S. Preuss, G. Jander, Arabidopsis NATA1 acetylates putrescine and decreases defense-related hydrogen peroxide accumulation, *Plant Physiol.* 171 (2016) 1443–1455.

[35] H. Mo, X. Wang, Y. Zhang, G. Zhang, J. Zhang, Z. Ma, Cotton polyamine oxidase is required for spermine and camalexin signalling in the defence response to *Verticillium dahlia*, *Plant J.* 83 (2015) 962–975.

[36] P. Tavladoraki, M.N. Rossi, G. Saccuti, M.A. Perez-Amador, F. Polticelli, R. Angelini, R. Federico, Heterologous expression and biochemical characterization of polyamine oxidase from Arabidopsis involved in polyamine back conversion, *Plant Physiol.* 141 (2006) 1519–1532.

[37] P. Fincato, P.N. Moschou, V. Spedaletti, R. Tavazza, R. Angelini, R. Federico, K.A. Roubelakis-Angelakis, P. Tavladoraki, Functional diversity inside the Arabidopsis polyamine oxidase gene family, *J. Exp. Bot.* 62 (2011) 1155–1168.

[38] F.R. Rossi, M. Marina, F.L. Pieckenstain, Role of arginine decarboxylase (ADC) in *Arabidopsis thaliana* defence against the pathogenic bacterium *Pseudomonas viridiflava*, *Plant Biol.* 17 (2015) 831–839.

[39] J.M. Vilas, F.M. Romero, F.R. Rossi, M. Marina, S.J. Maiale, P.I. Calzadilla, F.L. Pieckenstain, O.A. Ruiz, A. Gárriz, Modulation of plant and bacterial polyamine metabolism during the compatible interaction between tomato and *Pseudomonas syringae*, *J. Plant Physiol.* 231 (2018) 281–290.

- [40] C. Liu, K. E. Atanasov, A. F. Tiburcio, R. Alcazar, The polyamine putrescine contributes to H<sub>2</sub>O<sub>2</sub> and *RbohD/F*-dependent positive feedback loop in Arabidopsis PAMP-triggered immunity, *Front. Plant Sci.* 10 (2019) 1-12.
- [41] G.H.M. Sagor, S. Zhang, S. Kojima, S. Simm, T. Berberich, T. Kusano, Reducing cytoplasmic polyamine oxidase activity in Arabidopsis increases salt and drought tolerance by reducing reactive oxygen species production and increasing defense gene expression, *Front. Plant Sci.* 7 (2016) 214.
- [42] X. Zarza, K.E. Atanasov, F. Marco, V. Arbona, P. Carrasco, J. Kopka, V. Fotopoulos, T. Munnik, A. Gómez-Cadenas, A.F. Tiburcio, others, Polyamine oxidase 5 loss-of-function mutations in *Arabidopsis thaliana* trigger metabolic and transcriptional reprogramming and promote salt stress tolerance, *Plant. Cell Environ.* 40 (2017) 527–542.
- [43] L. Recalde, A. Vázquez, M.D. Groppa, M.P. Benavides, Reactive oxygen species and nitric oxide are involved in polyamine-induced growth inhibition in wheat plants, *Protoplasma.* 255 (2018) 1295–1307.
- [44] D. Walters, Resistance to plant pathogens: possible roles for free polyamines and polyamine catabolism, *New Phytol.* 159 (2003) 109–115.
- [45] N. Sewelam, N. Jaspert, K. Van Der Kelen, V.B. Tognetti, J. Schmitz, H. Frerigmann, E. Stahl, J. Zeier, F. Van Breusegem, V.G. Maurino, Spatial H<sub>2</sub>O<sub>2</sub> signaling specificity: H<sub>2</sub>O<sub>2</sub> from chloroplasts and peroxisomes differentially modulates the plant transcriptome differentially, *Mol. Plant.* 7 (2014) 1191–1210.
- [46] J. Morales, Y. Kadota, C. Zipfel, A. Molina, M. A. Torres. The Arabidopsis NADPH oxidases *RbohD* and *RbohF* display differential expression patterns and contributions during plant immunity, *J. Exp. Bot.* 67 (2016) 1663-1676.
- [47] E. Kámán-Tóth, T. Dankó, G. Gullner, Z. Bozsó, L. Palkovics, M. Pogány, Contribution of cell wall peroxidase- and NADPH oxidase-derived reactive oxygen species to *Alternaria brassicicola*-induced oxidative burst in Arabidopsis, *Mol. Plant Pathol.* 20 (2019) 485–499.
- [48] R. Mittler, ROS are good, *Trends Plant Sci.* 22 (2017) 11–19.
- [49] A.I. Chávez-Martínez, F.I. Jasso-Robles, M. Rodríguez-Kessler, S.S. Gill, A. Becerra-Flora, J. F. Jiménez-Bremont, Down-regulation of arginine decarboxylase gene-expression

results in reactive oxygen species accumulation in Arabidopsis, *Biochem. Biophys. Res. Commun.* 506 (2018) 1071–1077.

[50] Y.-Y. Du, P.-C. Wang, J. Chen, C.-P. Song, Comprehensive functional analysis of the catalase gene family in *Arabidopsis thaliana*, *J. Integr. Plant Biol.* 50 (2008) 1318–1326.

[51] D.C. Wilson, P. Carella, R.K. Cameron, Intercellular salicylic acid accumulation during compatible and incompatible *Arabidopsis-Pseudomonas syringae* interactions, *Plant Signal. Behav.* 9 (2014) e88608.

[52] H.-M. Yuan, W.-C. Liu, Y.-T. Lu, CATALASE2 coordinates SA-mediated repression of both auxin accumulation and JA biosynthesis in plant defenses, *Cell Host Microbe.* 21 (2017) 143–155.

[53] E. K. Jang, K. H. Min, S. H. Kim, S. H. Nam, S. Zhang, Y. C. Kim, B. H. Cho, K.Y. Yang, Mitogen-activated protein kinase cascade in the signaling for polyamine biosynthesis in tobacco, *Plant Cell Physiol.* 50 (2009) 658-664.

[54] D. Lu, S. Wu, X. Gao, Y. Zhang, L. Shan, P. He, A receptor-like cytoplasmic kinase, BIK1, associates with a flagellin receptor complex to initiate plant innate immunity, *PNAS* 107 (2010) 496-501.

[55] Y. Kadota, J. Sklenar, P. Derbyshire, L. Stransfeld, S. Asai, V. Ntoukakis, J. D. G. Jones, K. Shirasu, F. Merke, A. Jones, C. Zipfel, Direct regulation of the NADPH oxidase RBOHD by the PRR-Associated Kinase BIK1 during plant immunity, *Mol. Cell* 54 (2014) 43-55.

[56] P. Lariguet, H.E. Boccacandro, J.M. Alonso, J.R. Ecker, J. Chory, J.J. Casal, C. Fankhauser, A growth regulatory loop that provides homeostasis to phytochrome A signaling, *Plant Cell.* 15 (2003) 2966–2978.

[57] A.N.A. Rodrigo-Moreno, N. Andrés-Colás, C. Poschenrieder, B. Gunsé, L. Peñarrubia, S. Shabala, Calcium- and potassium-permeable plasma membrane transporters are activated by copper in Arabidopsis root tips: linking copper transport with cytosolic hydroxyl radical production, *Plant. Cell Environ.* 36 (2013) 844–855.

## Figure Legends

**Fig. 1.** Polyamine oxidase gene expression and enzymatic activity in *A. thaliana* seedlings infected with *Pst*. Total PAO activity was estimated by pink adduct production at 515 nm in 15-day-old *A. thaliana* Col-0 seedlings 0, 24, 48 and 72 hpi with *Pst* using Spd (A) and Spm (B) as substrates for amine-oxidation. Data were transformed into H<sub>2</sub>O<sub>2</sub> molar concentrations using the molar extinction coefficient ( $2.6 \times 10^4 \text{ M}^{-1} \text{ cm}^{-1}$ ). Values are means  $\pm$  SE of three replicates. Asterisks indicate values that differ at  $p \leq 0.05$  (\*),  $p \leq 0.01$  (\*\*) and  $p \leq 0.001$  (\*\*\*) between inoculated and non-inoculated plants at the indicated time points (h) according to Student's T test. (C) Real-time RT-PCR analysis of *AtPAO1*, *AtPAO2*, *AtPAO3*, *AtPAO4*, and *AtPAO5* genes in 15-day-old *A. thaliana* ecotype Col-0 seedlings 0, 24, 48 and 72 hpi with *Pst*. Gene expression values were normalized to the *AtEF1 $\alpha$*  reference gene and relative to non-inoculated plants using the  $2^{-\Delta\Delta\text{Ct}}$  method. Values are means  $\pm$  SE of three replicates. Asterisks indicate values that differ at  $p \leq 0.05$  (\*),  $p \leq 0.01$  (\*\*) and  $p \leq 0.001$  (\*\*\*) according to Student's T test.

**Fig. 2.** Bacterial titers in Arabidopsis polyamine oxidase mutant lines infected with *Pseudomonas syringae*. Fifteen-day-old seedlings were inoculated with *Pst* and the number of colony forming units (CFU) was estimated 24, 48 and 72 hpi in the mutant lines *Atpao1-1* (A), *Atpao2-1* (B) and *Atpao1-1 x Atpao2-1* (C). Wild type *A. thaliana* ecotype Col-0 was used as a control. Values are means  $\pm$  SE of three replicates. Asterisks indicate values that differ at  $p \leq 0.01$  (\*\*) according to one-way ANOVA followed by Dunnett's test. Experiments were repeated twice obtaining similar results.

**Fig. 3.** Polyamine oxidase activity in *Atpao* mutant lines infected by *Pseudomonas syringae*. Polyamine oxidase activity was assessed in 15-day-old seedlings of A) *Atpao1-1*, B) *Atpao2-1* and C) *Atpao1-1 x Atpao2-1* mutant lines that were mock-inoculated (MgCl<sub>2</sub>) or *Pst* inoculated at 0, 24, 48 and 72 hpi using Spd (first column) or Spm (second column) as substrates for amine-oxidation. PAO activity was estimated by pink adduct production at 515 nm and data were transformed into H<sub>2</sub>O<sub>2</sub> molar concentrations using the molar extinction coefficient ( $2.6 \times 10^4 \text{ M}^{-1} \text{ cm}^{-1}$ ). Values are means  $\pm$  SE of three replicates. Asterisks indicate values that differ at  $p \leq 0.05$  (\*),  $p \leq 0.01$  (\*\*) and  $p \leq 0.001$  (\*\*\*)

between infected and non-inoculated *Atpao* mutant lines. Statistical analysis was performed at the indicated time points (h) according to Student's T test.

**Fig. 4.** Hydrogen peroxide production by *Atpao1-1*, *Atpao2-1* and *Atpao1-1 x Atpao2-1* mutant lines during the infection by *Pseudomonas syringae*. (A) The H<sub>2</sub>O<sub>2</sub> concentration was determined with the molar extinction coefficient at 515 nm ( $2.6 \times 10^4 \text{ M}^{-1} \text{ cm}^{-1}$ ) in 15-day-old-seedlings after 0, 24, 48 and 72 hpi. Values are means  $\pm$  SE of three replicates. Asterisks indicate values that differ at  $p \leq 0.05$  (\*) and  $p \leq 0.001$  (\*\*\*) between the *Atpao* mutant lines and the WT according to one-way ANOVA followed by Dunnett's test. (B) *In situ* H<sub>2</sub>O<sub>2</sub> production was analyzed 0, 24, 48 and 72 hpi in infected leaves of 15-day-old-seedlings by 3,3-diaminobenzidine staining. The H<sub>2</sub>O<sub>2</sub> signal is in brown color. Scale bar, 0.5 mm.

**Fig. 5.** Superoxide anion radical production by *Atpao1-1*, *Atpao2-1* and *Atpao1-1 x Atpao2-1* mutant lines infected by *Pseudomonas syringae*. (A) The O<sub>2</sub><sup>•-</sup> concentration was determined with the molar extinction coefficient at 515 nm ( $2.6 \times 10^4 \text{ M}^{-1} \text{ cm}^{-1}$ ) in 15-day-old-seedlings after 0, 24, 48 and 72 hpi. Values are means  $\pm$  SE of three replicates. Asterisks indicate values that differ at  $p \leq 0.05$  (\*),  $p \leq 0.01$  (\*\*),  $p \leq 0.001$  (\*\*\*), and  $p \leq 0.0001$  (\*\*\*\*) between the *Atpao* mutant lines and the WT according to one-way ANOVA followed by Dunnett's test. (B) *In situ* O<sub>2</sub><sup>•-</sup> production was detected in leaves of 15-day-old-seedlings by NBT staining 0, 24, 48 and 72 hpi. The O<sub>2</sub><sup>•-</sup> signal is in blue color. Scale bar, 0.5 mm.

**Fig. 6.** Determination of RBOH enzymatic activity in 15-day-old Arabidopsis *Atpao1-1*, *Atpao2-1* and *Atpao1-1 x Atpao2-1* mutant lines infected by *Pseudomonas syringae*. In-gel activity assay of RBOH was performed in a native gel with 300  $\mu\text{g}$  of protein extract. The gel was incubated in NADPH and NBT solution until the bands appeared. The graphs show total RBOH activity at 0 (A), 24 (B), 48 (C) and 72 (D) hpi. Values are means  $\pm$  SE of three replicates. Asterisks indicate values that differ at  $p \leq 0.05$  (\*) and  $p \leq 0.01$  (\*\*) between the *Atpao* mutant lines and the WT according to Student's T test.

**Fig. 7.** Estimation of CAT and SOD activity in 15-day-old Arabidopsis *Atpao1-1*, *Atpao2-1* and *Atpao1-1 x Atpao2-1* mutant lines infected by *Pseudomonas syringae*. (A) CAT

activity was calculated based on the rate of H<sub>2</sub>O<sub>2</sub> decomposition at 240 nm ( $\epsilon = 43.6 \text{ M}^{-1} \text{ cm}^{-1}$ ), in Col-0 and *Atpao* mutant lines inoculated and non-inoculated with *P. syringae*. Asterisks (\*) indicate values that differ at  $p \leq 0.05$  between the *Atpao* mutant lines and the WT according to one-way ANOVA followed by Dunnett's test. (B) In-gel activity of Mn-SOD, Fe-SOD and Cu-Zn-SOD in non-inoculated Col-0 and *Atpao* mutant lines. (C) In-gel activity of Mn-SOD, Fe-SOD and Cu-Zn-SOD in Col-0 and *Atpao* mutant lines 72 hpi with *Pst*. Asterisks (\*) indicate values that differ at  $p \leq 0.05$  between each SOD-isoforms (MnSOD, FeSOD, Cu/ZnSOD) in the *Atpao* mutant lines and the WT according to one-way ANOVA followed by Dunnett's test. Values are mean  $\pm$  SE of three replicates. The data are representative of two independent experiments with similar results.

**Fig. 8.** Polyamine oxidase activity contributes to ROS homeostasis through regulation of RBOH activity in the *Arabidopsis-Pst* interaction. Bacterial recognition by specific receptors (FLS2 and BAK1) triggers kinase (BIK1) phosphorylation, the activation of MAPK cascades and PA biosynthesis [11, 53, 54, 55]. The RBOH enzyme is activated by phosphorylation and the production of the O<sub>2</sub><sup>•-</sup> and H<sub>2</sub>O<sub>2</sub> increases [55]. MAPK-mediated signaling and H<sub>2</sub>O<sub>2</sub> derived from RBOH activity could induce *AtPAO1* and *AtPAO2* gene transcription. PAO activity augments, and the oxidation of Spm and Spd contribute to H<sub>2</sub>O<sub>2</sub> production. Hydrogen peroxide derived from PAO activity might have a specific role in plant defense depending on the subcellular compartment in which PAs are oxidized (peroxisome or cytosol). H<sub>2</sub>O<sub>2</sub> derived from the cytosol (yellow arrow) or the peroxisome (blue arrow) could have a differential effect on gene transcription and defense success, as described by others [45]. Put levels increase by *de novo* synthesis [38] and bacterial excretion to the apoplast [39]. In addition, Put increments could be the result of PA full back-conversion by PAO activity. We suggest the PAO activity is involved in RBOH activity negative regulation and contributes to the maintenance of ROS homeostasis. This figure was created with the help of BioRender (<https://biorender.com/>).

Figure 1.

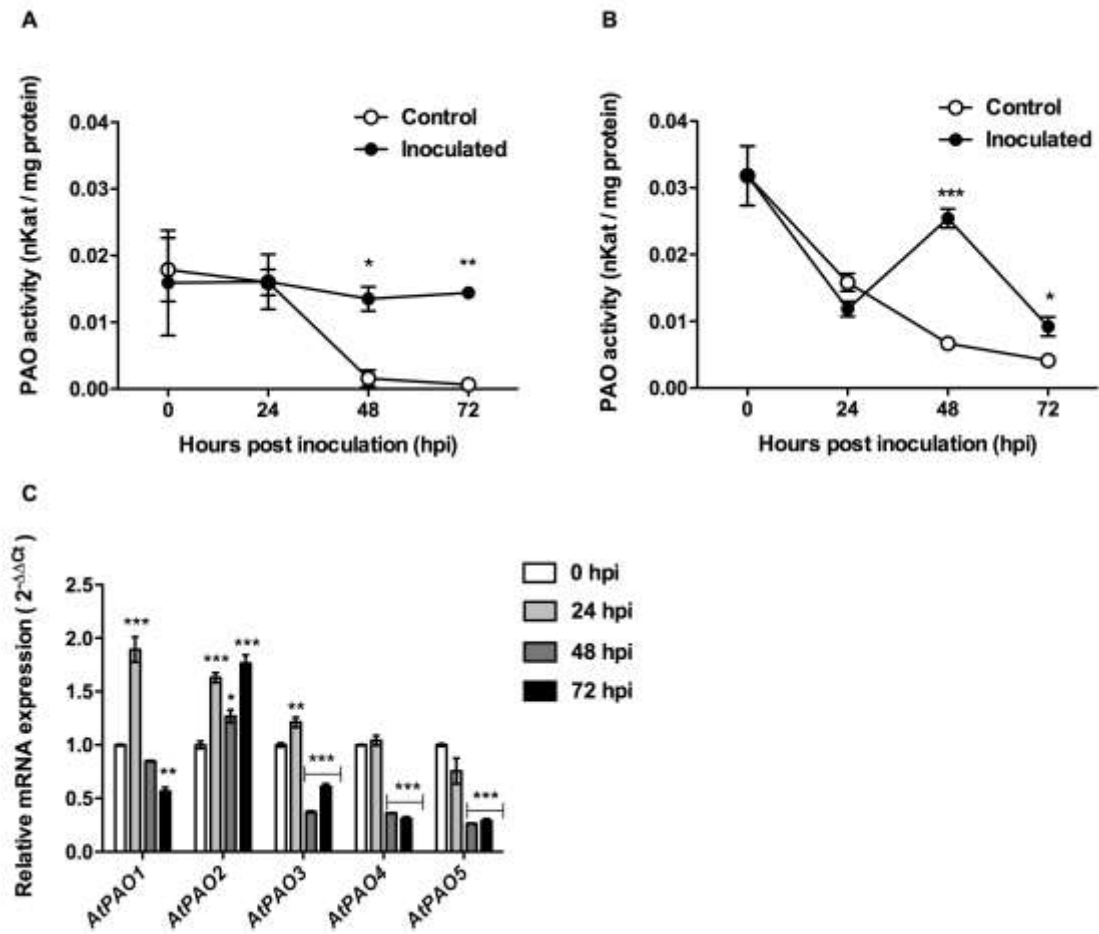


Figure 2.

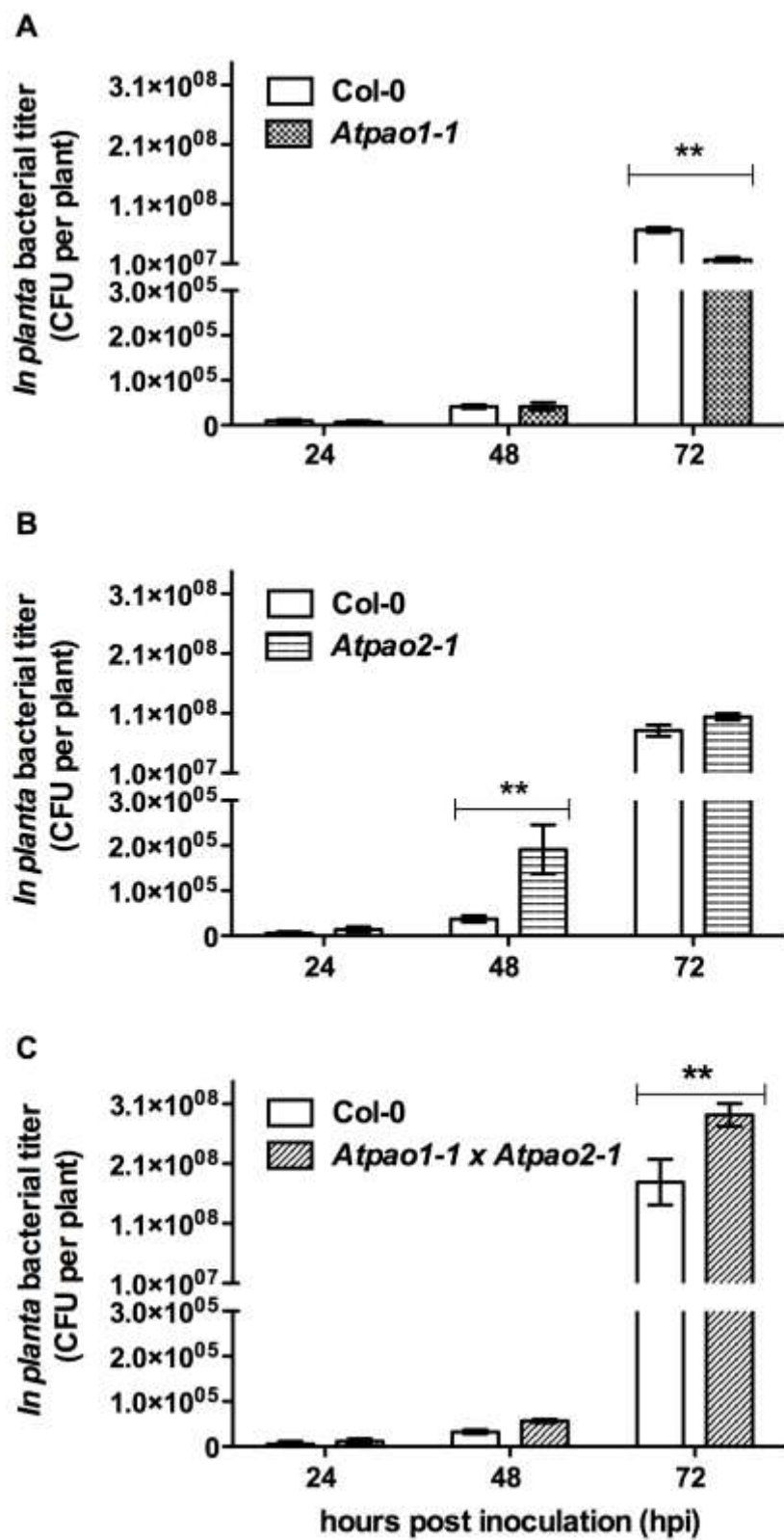


Figure 3.

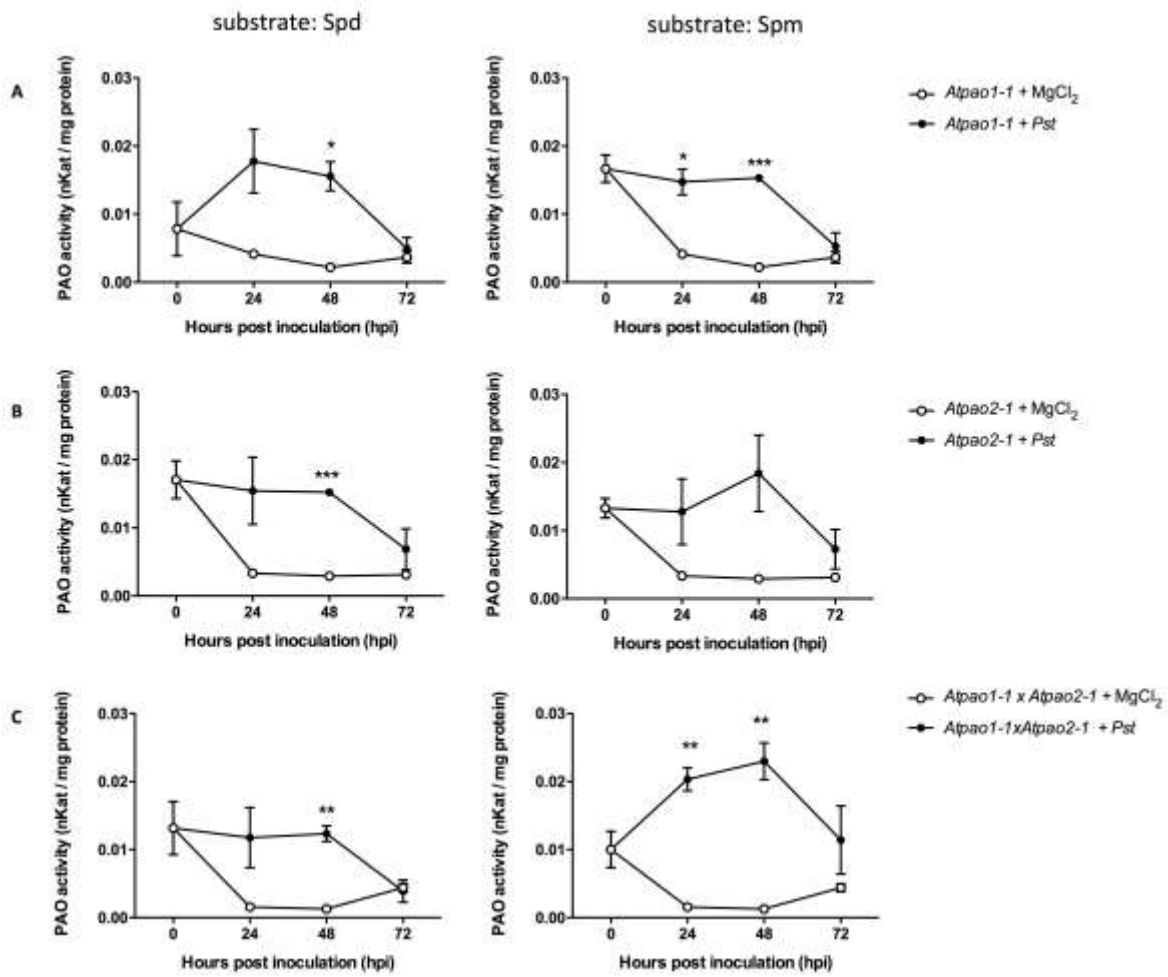


Figure 4.

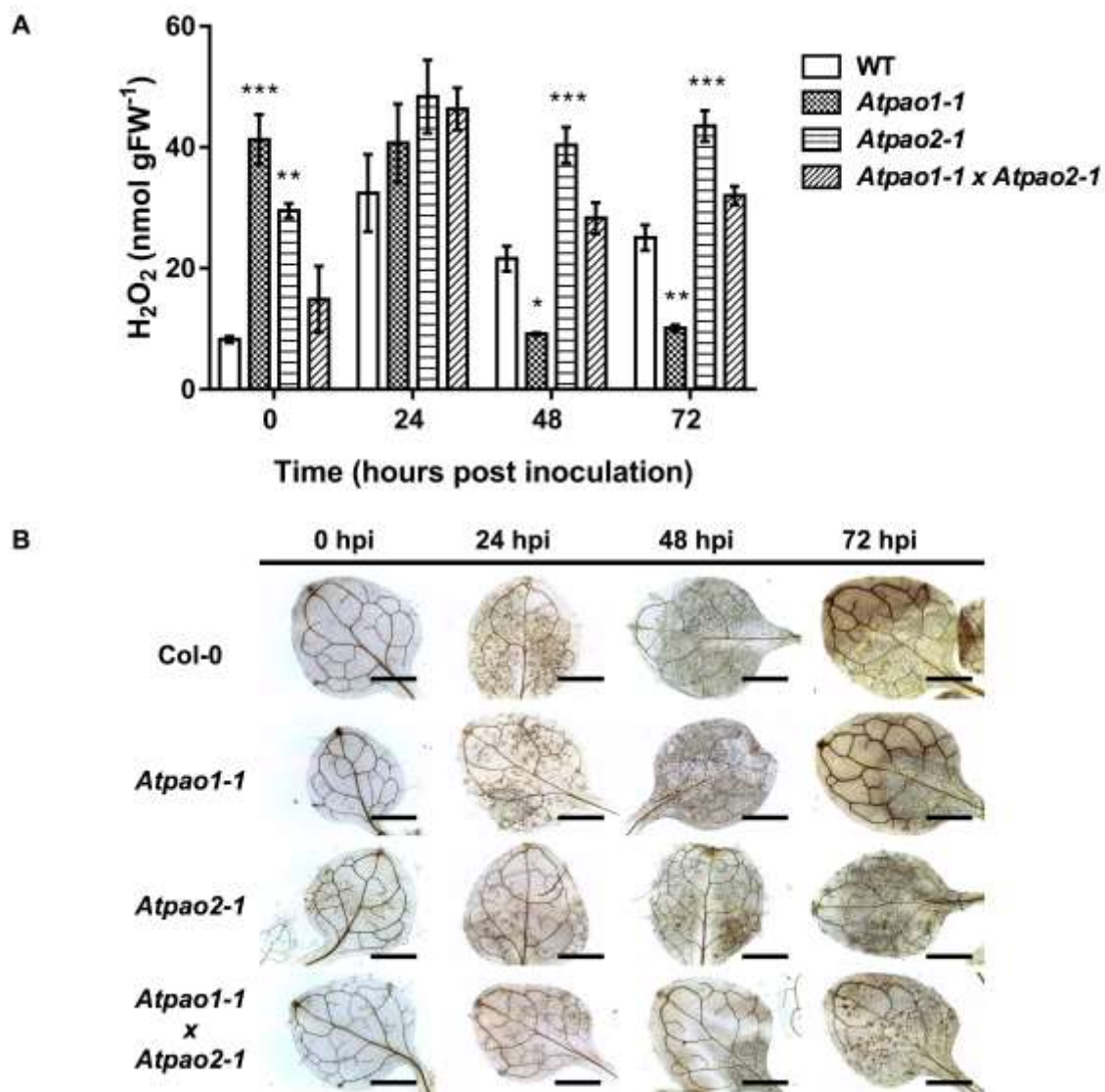


Figure 5.

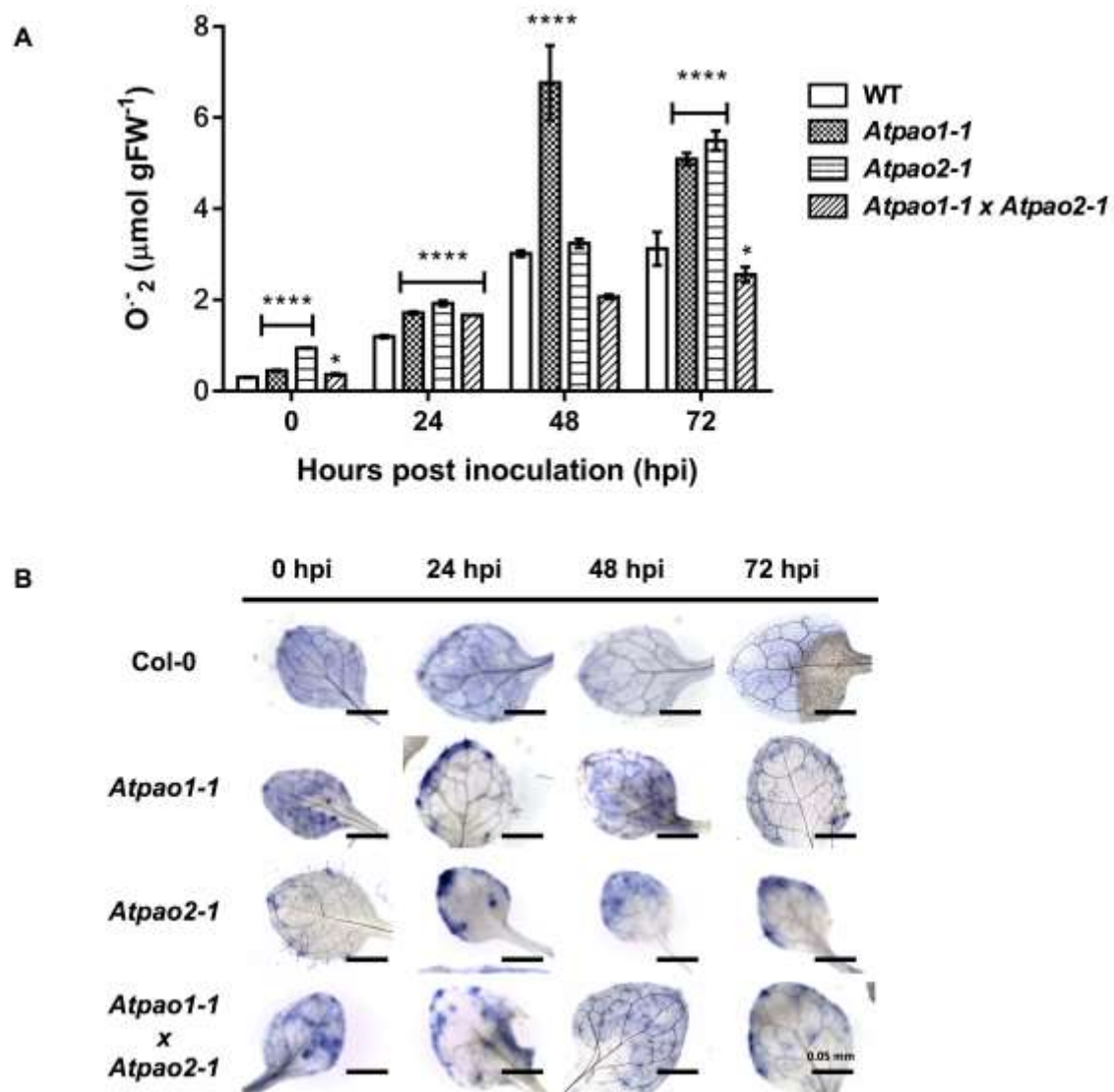


Figure 6.

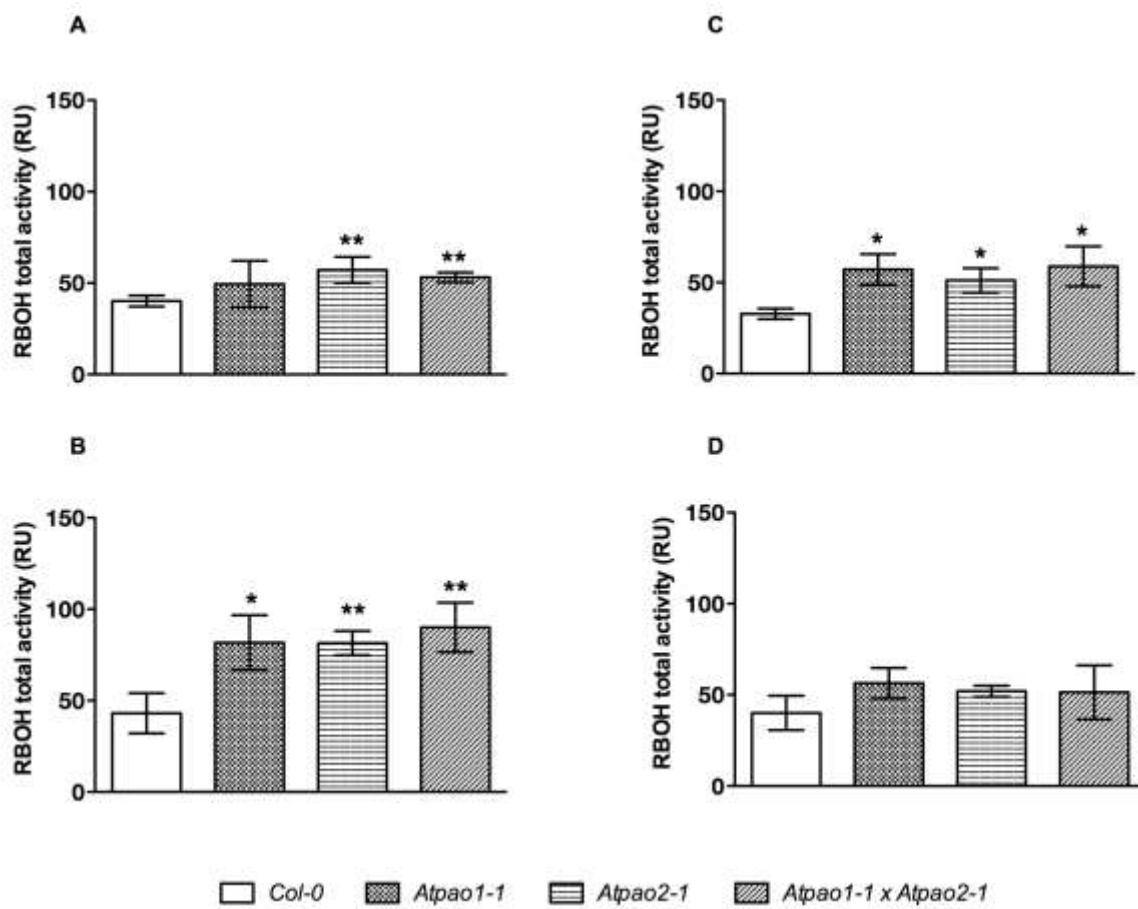


Figure 7.

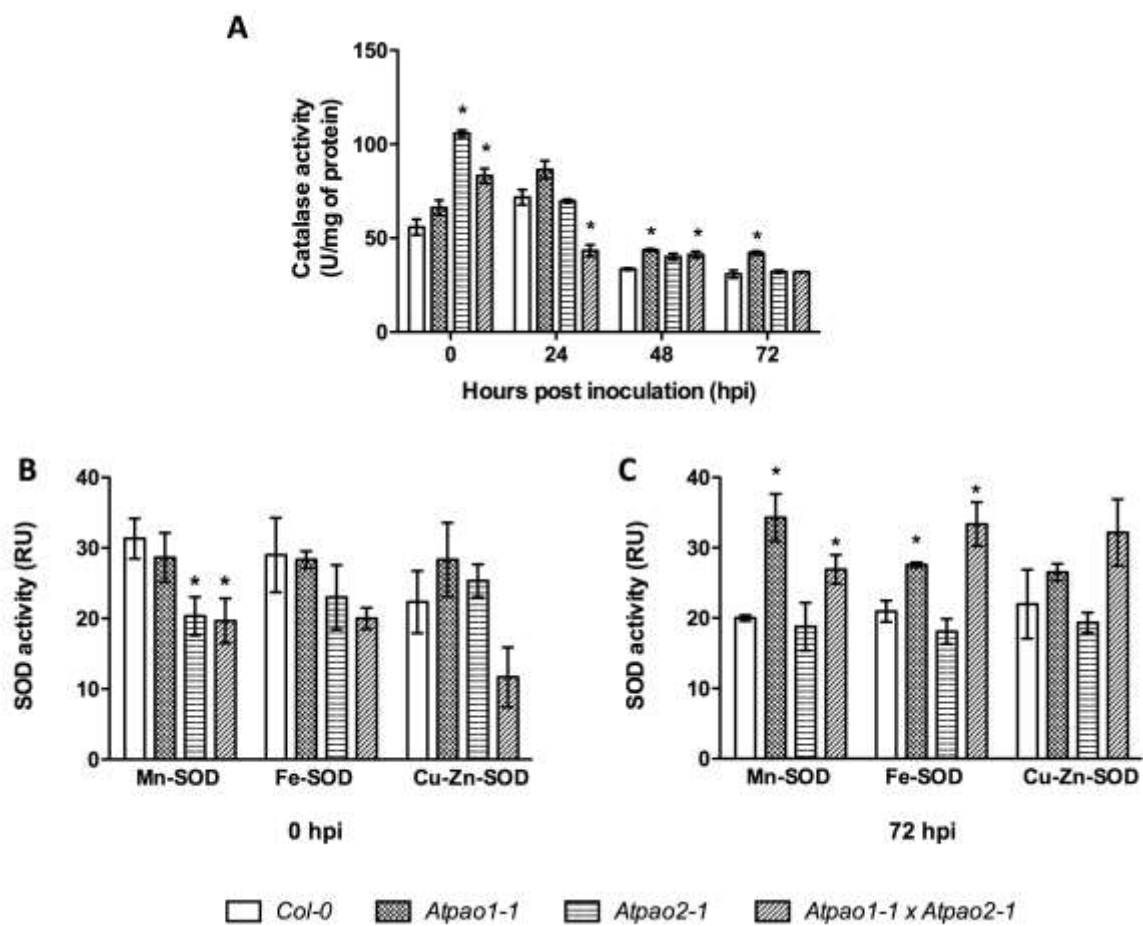


Figure 8.

